INSTITUT NATIONAL DE PHYSIQUE NUCLEAIRE
ET DE PHYSIQUE DES PARTICULES

LPNHE_Paris

L.P.N.H.E. 89 - 04

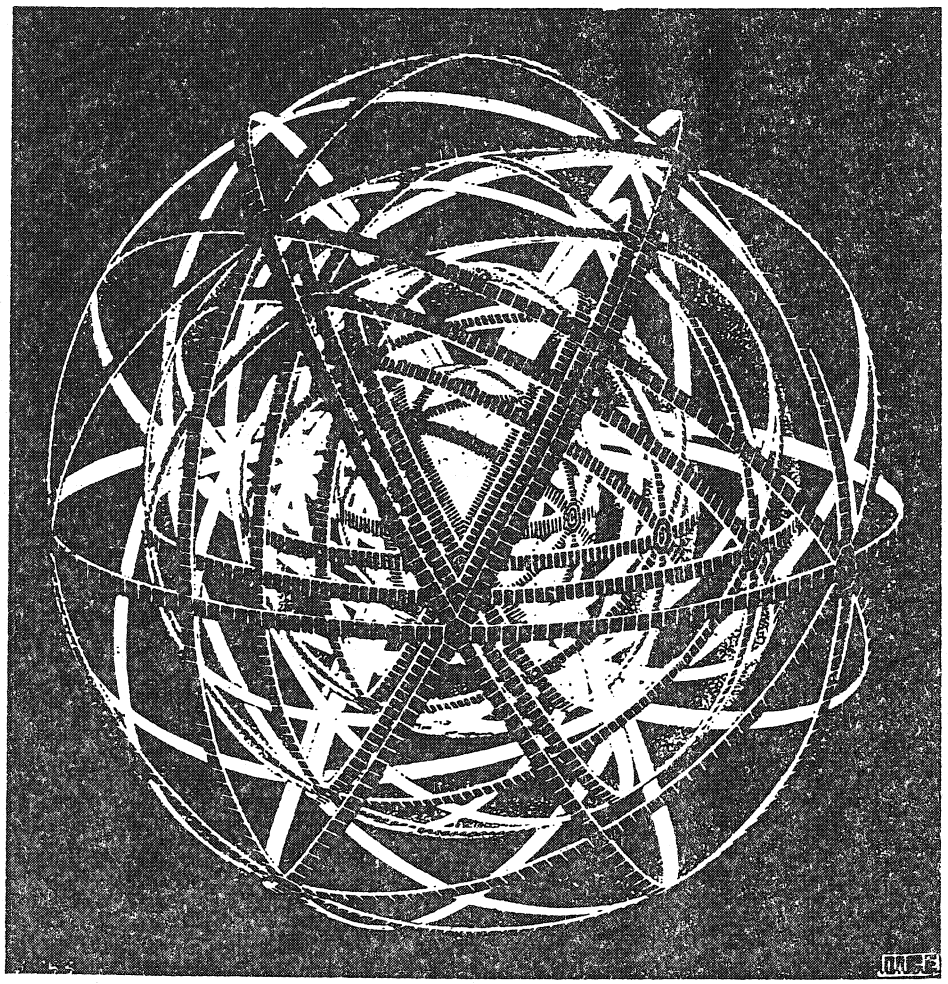

THE MULTISTEP CHAMBER AS A HARDWARE EVENT BUFFER

presented by
P. ASTIER

June 1989

UNIVERSITES PARIS VI ET PARIS VII

4 PLACE JUSSIEU - TOUR 33 - REZ-DE-CHAUSSEE - 75252 PARIS CEDEX 05

LABORATOIRE DE PHYSIQUE NUCLEAIRE ET DE HAUTES ENERGIES

June 1989

THE MULTISTEP CHAMBER AS A HARDWARE EVENT BUFFER

P. Astier[1], G. Charpak, W. Dominik[2] and F.Sauli
CERN, Geneva, Switzerland.

(presented by P. Astier)

Abstract: We study a multistep chamber optically read out used as a buffered tracking detector for a tagged neutrino beam.

Talk given at the
4th Pisa Meeting on Advanced Detectors,
La Biodola, Isola d'Elba, Italy, 21-25 May 1989.

[1]Now at Laboratoire de Physique Nucléaire et de Hautes Energies, IN2P3-CNRS/Universités Paris VI-VII, 4 place Jussieu, F-75252 Paris Cedex 05, France.
[2]On leave of absence from Warsaw University, Poland.

1 Introduction

We have investigated the possibility of using multistep chambers as part of a tagged neutrino beam. Such a setup can be shortly described as follows: in a standard narrow band beam, one equips the end of the decay tunnel to measure the position and the energy of the charged secondaries from meson decays, and to identify muons and electrons. This tunnel is followed by about 200 meters of shielding and a neutrino calorimeter. This kind of facility aims at detecting, for each neutrino interaction, the accompanying particle(s) produced in the meson decay: the flavor of the neutrino is thus tagged on an event by event basis. The physics opened by such a setup is described elsewhere [1], we just quote here the main constraints it should fulfill to equip the neutrino Narrow Band Beam at the CERN SPS (assuming a 2 s long spill):

- The flux reaches 10^5 to 10^6 m.i.p/s.cm^2 at the end of the decay tunnel; It falls very rapidly when going off axis. This flux is on the very high side of MWPC's capability considering pile-up and space charge effects. To get an acceptable tagging efficiency, the apparatus should cover a 1.2 m radius disk with possibly a 15 cm hole or dead region to let the meson beam through.
- The total rate on the tagging station is a few hundred MHz. As it is hopeless to record the whole information, the tagger should be read out only when a neutrino interaction occurs. The particle(s) produced with the neutrino hit the tagger long before the trigger signal reaches it; the tagging system should thus have a memory of the order of 2 μs allowing the neutrinos to reach the calorimeter, the trigger to be formed and sent back. Delaying thousands of channels of the tracking system with cables or electronic devices is not very appealing.

With its high rate capability and its built-in gaseous delay, the multistep chamber [2] is an appropriate choice for the tracking part of the system. It provides also a low sensitive mass (a few grams per m^2 of sensitive area), an interesting feature in a highly radioactive environement; multistep chambers finally accomodate a two dimensional optical readout which practically suppresses pile-up problems.

In this paper, we do not aim to propose a final design of a would-be tagging system. We only study a possible tracking subdetector to contribute both to the physics goal and to detector development.

2 Apparatus

2.1 Chamber

Our test chamber is a multistep parallel plate avalanche chamber made of successive crossed wire grids (50 μm wires spaced by 500 μm, 10x10 cm^2 in size) stretched on glass

fiber insulating frames. The grids are held at suitable potentials which define regions with different functions in the gas volume (fig. 1):
- a conversion region in which electrons released by charged particles (or eventually X rays in some lab tests) are collected,
- the first stage: a high field region where the collected electrons are preamplified in the parallel plate mode,
- a low-field drift (or transfer) region where part of the preamplifed electrons are tranferred and drift. The transfered fraction can be estimated by the electric fields ratio:$E_{transfer}/E_{preamp.}$[3] and lies around 10% for our voltage settings.
- the second stage is again a high field region where the preamplified and transfered electrons are finally amplified. The gating electrode (or gate), located just before the second stage cathode can block or let the drifting electrons through.

The delay provided by the chamber is fixed by the transfer section length (11 cm) and the drift velocity (around 5 cm/μs for most of the gas mixtures): 2.2 μs are available for the trigger signal to come back and command the opening of the gate. This gate is made of 50 μm parallel wires spaced by 1 mm; odd and even wires are connected together to form two groups of wires whose voltage difference drives the gate transparency (fig. 2): the gate is normally closed (150 V is used as a blocking voltage) but when a trigger comes, a 150 V pulse brings the difference near zero and the electron cloud passes through to the second stage. In this mode of operation, the positive ions from the avalanches in the second stage are collected on the gate and do not disturb the electric field upwards. The gate potential is to be chosen to equate the electric fields upwards and downwards in order to maintain straight field lines in the gate vicinity. We used a home made pulser with 5 ns rise time and 10 ns fall time. Minimum workable width was 30 ns.

2.2 Gas filling and read out

It has been shown that the addition of some vapours (among which some photosensitive compounds and water) in the gas mixture results, under avalanche conditions, in copious light emission in or close to the visible region[4]. The amount of light produced increases with vapour concentration up to a plateau in the range of 1 photon per electron. Among such vapours tetrakis(dimethylamine)ethylene (TMAE) and triethylamine (TEA) have been extensively studied [5]. TMAE emits in the green, around 480 nm, but has the practical inconvenience of a low vapour pressure (0.4 Torr at room temperature) which obliges to heat the detector to reach an acceptable scintillation yield. The relatively high vapour pressure of TEA (52 Torr at 20°C) is counterbalanced by its emission in the close ultraviolet range (peaked at 280 nm). We used TEA as light emitter (in an argon-methane mixture) for practical convenience (no heating necessary and TEA does not react with air), and we converted its emission to visible, placing a thin wavelength shifter (WLS) foil against the last grid [8]. As UV light is emitted close to this grid, the reemmited light is not too much spread out by this trick. To also allow direct imaging of UV light, the chamber window was made of Aclar (polychlorotrifluoroethylene or PCTFE), a plastic reasonably transparent in the close

UV region.

The emitted light can be detected by a commercially available solid-state Charge Coupled Device (CCD) video camera, preceeded by an objective and an image intensifier. The intensifier spectral sensitivity must match the emitted wavelengths as well as the lens and chamber window transparencies. This requirement restricts the choice for UV read out but is relaxed if one uses the wavelength shifter foil. The light loss in the conversion (about one half due to isotropic emission of shifted light) is then more than compensated by the greater aperture of available visible light objectives (f/1 for visible light and f/4.5 quartz optics for UV light). The image intensifiers now include a gating capability down to a few nanoseconds, and reduce the recorded photocathode noise to practically zero.

If CCD's reach the mega-pixel range, their maximum read out speed capability is nowadays 50 Hz when driven by standard video electronics, and a factor of 2 or 3 faster with a dedicated driving sheme. This would probably be sufficient for the neutrino tagging application. But as some particle physics applications need both fine grained and fast readout [6], some improvement in this field is anyway to be expected in the coming years.

3 Operation characteristics

3.1 Charge and light yields

The charge gain was measured using a two-channel charge amplifier connected to the cathodes of the amplifying stages, with an integration time around 1 μs. Thus the charge signal recorded does not include the positive ions contribution. It is related to the input charge by $Q_{measured} \simeq (M/Ln(M))Q_{input}$[7], Where M is the actual multiplication factor and Q_{input} the charge of electrons released in the conversion space. The ratio $Q_{measured}/Q_{input}$ is often called "practical gain" and we will call it gain in what follows.

The light yield was measured using an RCA 8850 photomultiplier tube calibrated on the single and double photoelectron peaks of the output charge spectrum. As the inferred number of photons emitted relies on a computation using solid angle acceptance, photocathode area and quantum efficiency, and assumes phototube linearity over two decades, the results are to be taken within a factor of 2. The phototube pulse shape does not show any evidence for long lived excited states of TEA resulting in delayed light emission.

The first stage gain can reach 10^4 in an Ar-CH_4-TEA mixture for any methane concentration between 0 and 17% and 2% TEA. The gain slope (with respect to high voltage) decreases with increasing methane concentration. The light output was found to stay proportional to charge (around 1.5 photon per "practical" electron) when varying both high voltage and methane concentration. The energy resolution (measured

at 5.9 keV) was found around 25% (FWHM) using charge collection and 30% using light; these resolutions include some 10% gain variations on the chamber area. The second stage has similar characteristics when operated alone; its gain is limited to a few hundred when the whole chamber is on in open-gate (or DC) mode, and reaches 3.10^3 in pulsed (or AC) mode. Taking into account the 10% transferred charge fraction the overall gain can reach more than 10^6. The practical high voltage limitation arises from sparking, a universal tendency of parallel plate avalanche chambers, which can be reduced by a careful design insisting upon the grids beeing parallel to a high accuracy.

3.2 Delay characteristics

The neutrino tagging application needs an accurate definition of the chamber delay; in case of poor timing at the end of the transfer, a wide gating pulse would have to be applied, and many events would then be transferred to the second stage and read out, increasing the difficulty to associate the right candidate with the downstream neutrino interaction. Long term fluctuations of the delay can certainly be monitored, using e.g. laser induced ionization; statistical fluctuations from event to event must be taken into account in the final design.

One measurement was carried out using 5.9 keV X-rays, each cathodes being connected to a preamplifier-discriminator [9], the outputs of which fed a time to amplitude converter, the first stage as the t_0 and the second as the stop. The chamber was operated DC in order to measure its intrinsic delay and not depend on the gate circuit timing properties. The time jitter is 14 ns FWHM for a nominal delay of 2.45 μs. This measurement using a localized charge deposition accounts for the electron cloud spread in the transfer. Variations of the mean delay over the chamber area were found under 3 ns.

In the case of minimum ionizing particles, the electron cloud used for detection is as long as the conversion section (6 mm in our case); the light emission will hence last at least as long as the time necessary to collect this cloud ($\sim$ 120ns). We measured the delay spectrum of the chamber for m.i.p using scintillators slabs for the t_0 and a phototube to measure the time of the light pulse, its discriminated output being used as the stop. The peak is then 35 ns (FWHM) wide, still measured in DC mode. The same measurement as before gives about the same precision. The charge delocalization clearly worsens the delay accuracy with respect to 5.9 keV X-rays.This measurements refer to the leading edge jitter of the light or charge pulse and not to their duration.

The figure of merit of this chamber used as a hardware event buffer is the curve of chamber efficiency (using light output) versus gating pulse delay : it describes the probability to detect a particle off time with respect to the neutrino interaction. Considering the cloud length (120 ns) and the gate width (50 ns), one should expect a $\sim$ 150 ns efficiency curve width. Because of technical limitations, we resorted to counting the light pulses within a 100 ns gate and we found a 250 ns width (fig. 3) which includes the counting gate width. The actual memory time is thus of the order of 150 ns as could be checked practically in the test beam described below when tuning the

gate delay. Narrowing the gate under 50 ns decreases the efficiency without reducing much the memory time. Reducing the conversion gap thickness to 3 mm would narrow the memory (down to about 100 ns) and would adapt the gate and cloud length. In the sketched tagged neutrino beam, the gate would then select about 25 candidates per neutrino interaction. A precise time measurement (even with a poor granularity) would then be necessary to sort out the right one, which must anyway fulfill the kinematical constraints of the meson decay (mass and momentum).

3.3 Position accuracy

The position accuracy was measured in the CERN PS T7 test beam, using the setup sketched in fig 4. The vertical position of incident 5 GeV pions was measured using two microstrips plane having 60 μm pitch. With horizontal gate wires, we expect the worst position resolution to be obtained in the vertical direction because of unavoidable electrostatic distortions around the wires of the gate. The second stage of the chamber was imaged in a mirror by a gatable image intensifier coupled to a CCD camera [10]. The mirror reflectivity ranges from 0.80 at 250 nm to 0.87 in the visible range. We used a 105 mm f/4.5 quartz lens for UV readout (i.e. without a W.L.S. foil), and a 50 mm f/1 for visible light readout; both were used at full aperture. A phototube (RTC 8850) was set up beside the camera to monitor in a simple way the light output. The distance from chamber to camera and phototube was 70 cm. We tested three operation modes described below.

The trigger signal was the coincidence of three scintillators aligned with the microstrips. It was used to initiate the acquisition process, and delayed by about 2 μs to trigger the gates of the chamber and of the image itensifier. The major noise source in the images appeared to be due to the light emitted by the numerous particles going through the first stage of the chamber during the 20 ms video cycle, rather than photocathode noise which can be easily cut out while preserving the signal. Gated operation of the image intensifier (which consists in driving the photocathode bias) cuts both of them. A 30 ms inhibition was introduced in the trigger to avoid recording more than one track within the same video cycle (20 ms).

Data acquisition was performed by means of a Valet-plus system [11] reading out and writing on tape the ADC's of the microstrips, the ADC of the monitoring phototube, and the video signal from the camera (consisting essentially in a chain of electric pulses proportional to the pixel charge content) digitized on a commercially available 8 bit digitizer. The digitized video output was zero suppressed by software because the light spots hit typically a few hundred pixels among the 30 thousand pixels of the CCD (see fig 5). The acquisition rate was limited by the available memory in the digitizer (4 images) and the speed of the zero suppression loop. With a hardware zero suppression at digitization time, the acquisition rate would be limited by CCD scanning speed, which allows at least 50 images/s. The video signal was split between the digitizer and a TV screen which allowed to monitor by eye the chamber operation.

The vertical track positions in the microstrips and in the chamber were computed

by using a center of gravity method. This computation involved approximately 3 strips per microstrips plane and 20 CCD lines. The residual distribution (fig 6a) exhibits a 0.8 mm resolution (FWHM) for the three gas and read out conditions tested (see table 1).

We used the root mean square of the light spatial distribution as a spot size estimator (fig. 6b). The mean values quoted in the table show that using the W.L.S enlarges the spots by 20 to 30 %. The double track separation capability of the device (depending on a specific pattern recognition algorithm) can certainly lie in the range of 2 to 3 mm.

The light yield was measured with the phototube and expressed in number of photoelectrons (fig. 6c). The numbers in table 1 show an increase when using methane as the main quencher; actually, adding methane enables higher gains before breakdown under beam conditions.

Table 1

Gas filling	Position accuracy (FWHM) mm	light spot size (σ) mm	light output ($ph.e^-$ in PMT)
Ar methane (7%) TEA (2%) No WLS	0.8	1.25	-
Ar methane (7%) TEA (2%) With WLS	0.8	1.6	1200
Ar TEA (5%) With WLS	0.8	1.4	660

The inefficiency was estimated as the fraction of events having an integrated intensity of the digitized video signal under a given threshold (10 % of the mean signal from m.i.p). The raw result is 5%, from which 3% are due to trigger falling in a "dead" part of video cycle. The intrinsic inefficiency of the chamber can then be evaluated to 2%. The dead time in the video cycle can be removed by using a more sophisticated sheme for driving the CCD than the one used in the video mode.

4 Conclusions

If one discards the direct UV readout for practical reasons (need for a specially ordered image intensifier with enhanced UV sensitivity and UV lens), the chamber is to be operated with shifted light readout and Ar-methane-TEA gas filling. If the camera sits three times farther from the chamber (i.e. 2 m), the total collected light will decrease by a factor of ten and lie in the manageable range of one hundred photoelectrons, regarding efficiency and resolution; the light collected per pixel will not vary (as long as the spot hits a few pixels). The spatial resolution of our setup is certainly not limitated by the readout granularity but by the scale of electrostatic distortions around the meshes and the gate. Reducing the wire pitch of the gate to 0.5 mm seems hard to achieve for an area in the square meter range. The figure obtained here (0.8 mm) is anyway more than sufficient for the neutrino tagging application.

The memory time can reasonnably be hoped in the 100 ns range or even below with a 3 mm conversion. This is too long for the neutrino tagging, but this experiment would anyway need a precise timing measurement to associate particles from the same decay (especially for the K_{e3} decay) in order to reduce mistag rate (i.e. wrong particle(s) associated with a neutrino having interacted). This timing could then be used to refine the selection performed by the gating sheme.

This work was made possible by the technical help from R. Bouclier, J. Dupont and J.C. Santiard.

References

[1] Proposal for neutrino experiments at the IHEP accelerator using a tagged neutrino beam and a liquid argon detector, INFN(Pisa)- IHEP(Zeuthen)- JINR(Dubna)- IHEP(Serpukhov).

[2] A. Breskin et al., Nucl. Instr. and Meth. 178, 11, 1980. and references therein.

[3] A. Breskin et al., Nucl. Instr. and Meth. 161, 19, 1979.

[4] F. Sauli et al., proceeding of IEEE Nuclear Science Symposium, 1988, preprint CERN-EP/88-147, and references therein.

[5] M. Susuki et al., Nucl. Instr. and Meth. A254, 556, 1987.
G. Charpak et al, Nucl. Instr. and Meth. A269, 142, 1988.

[6] see e.g. D'Ambrosio et al., CERN-EP 89-44.

[7] J.R. Hubbard et al., Nucl. Instr. and Meth. 176, 233, 1980.

[8] 100 μm of doped polystyrene, made by M. Bourdinaud, DPhPE, CEN Saclay, France.

[9] J.C. Santiard, EP Internal Report 82-04.

[10] The CCD used was a 144x208 pixels matrix of size 4.32*5.82 mm^2 (Thomson 7852) driven by standard video electronics. We used a multichannel plate gatable image intensifier, 18 mm in diameter with a S20 photocathode and P36 fast phosphore screen (RTC XX 1410/SP 41721.160); A DEP electrostatic demagnifier reduces the image from 18 to 7 mm to match the diagonal size of the CCD.

[11] The Valet system is an acquisition package, developed at CERN, operating on a 68000 processor (or its younger brothers) sitting in a VME crate interfaced with CAMAC.

[12] For the study of noise in image intensifiers see e.g. the contribution by G. Penso in these proceedings.

List of Figures

1 Schematic transverse view of the chamber. 10

2 Gate transparency as a function of voltage difference between the two groups of wires. The 30 V long plateau around zero difference allows a rough setting of the opening pulse amplitude. 11

3 Chamber efficiency versus variation of the delay of the gating pulse around its nominal value 12

4 Sketch of the test beam setup for position accuracy measurement. A: chamber- B: camera- C: phototube- D: mirror (aluminized mylar foil)- E: microstrips planes- F: dark box. 13

5 A typical light spot drawn as a lego plot. The height represents the pixel brightness; the horizontal scale is in mm measured on the chamber. The small satellites around the spot are probably due to backscattered electrons on the phosphor screen of the image intensifier [12]. 14

6 Distributions from test beam analysis with Ar-methane-TEA gas filling and WLS foil: position residual (a), r.m.s of spots (b), light output in number of photoelectrons in PMT (c). 15

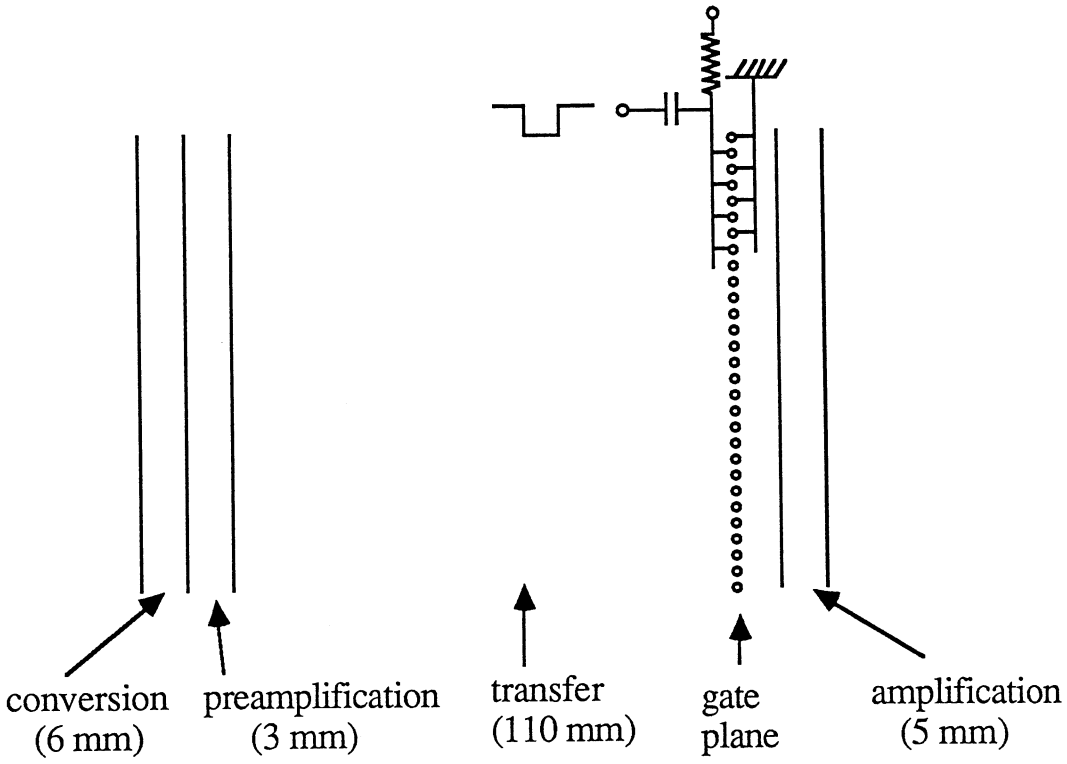
conversion
(6 mm)
preamplification
(3 mm)
transfer
(110 mm)
gate
plane
amplification
(5 mm)

Figure 1

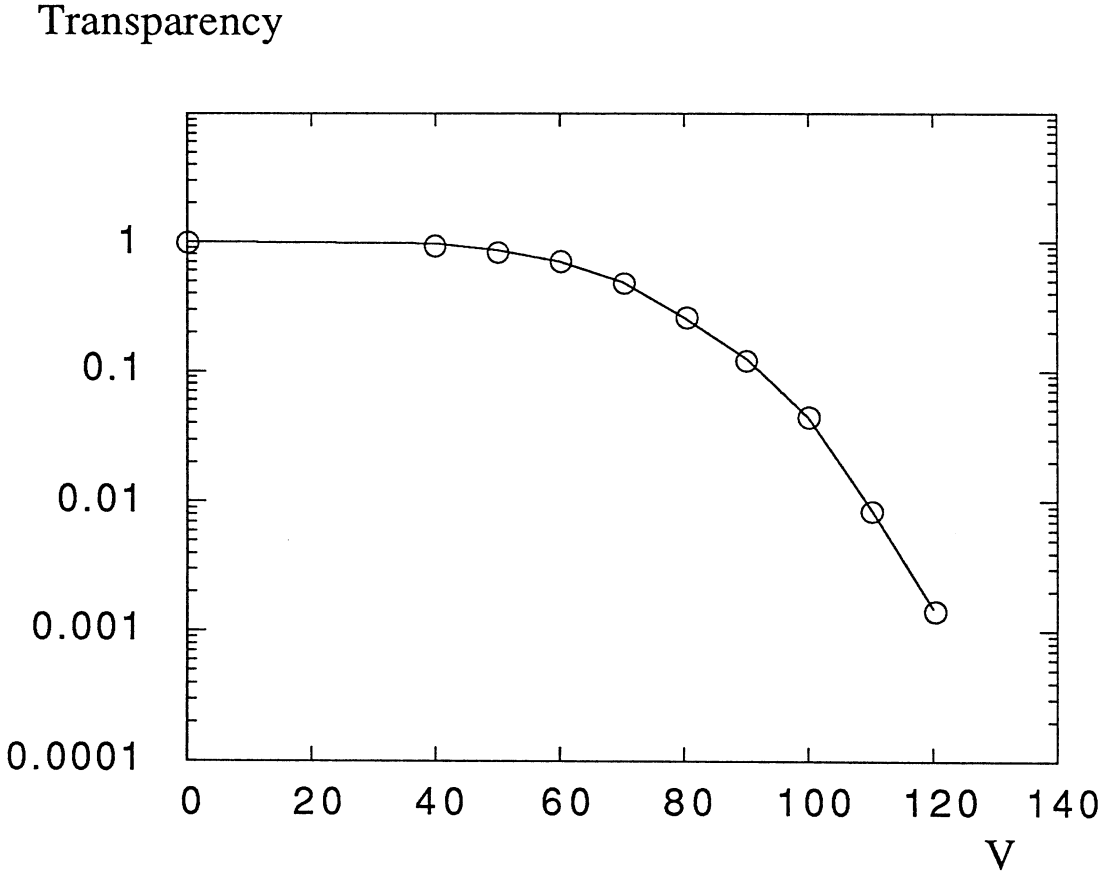

Figure 2

Efficiency

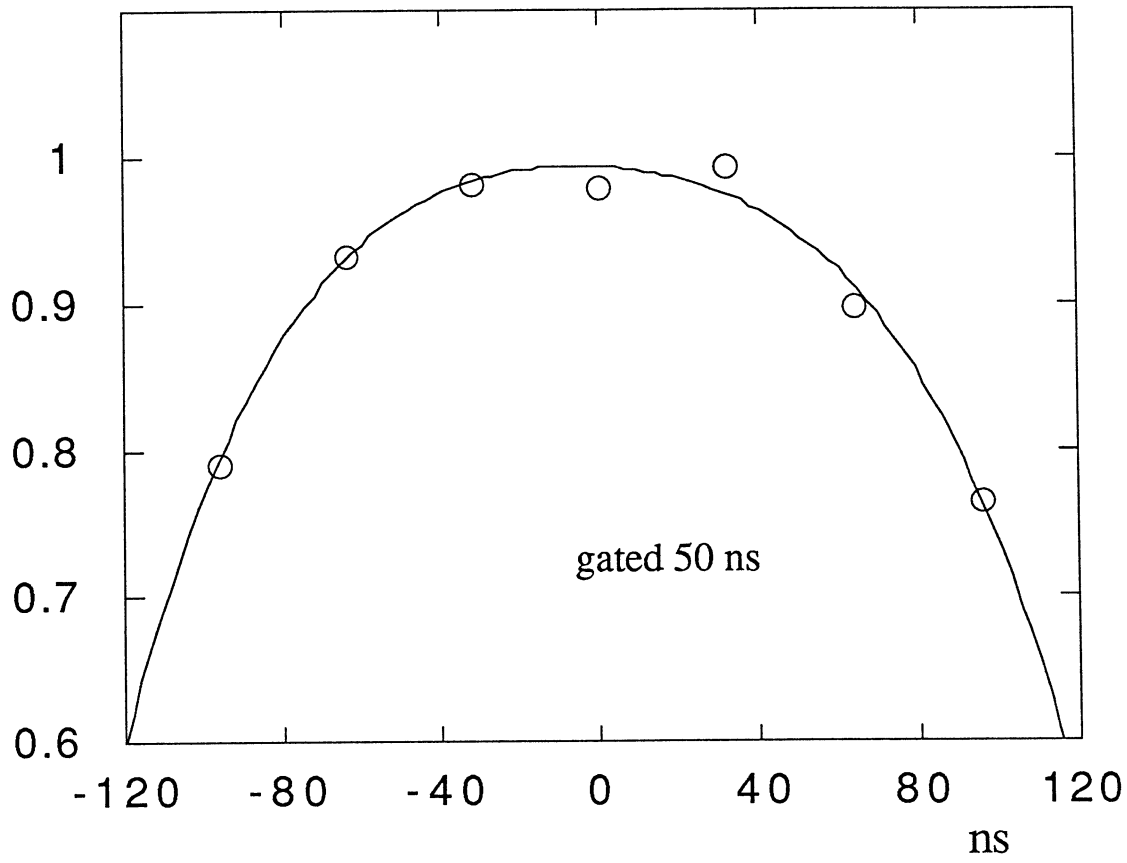

Figure 3

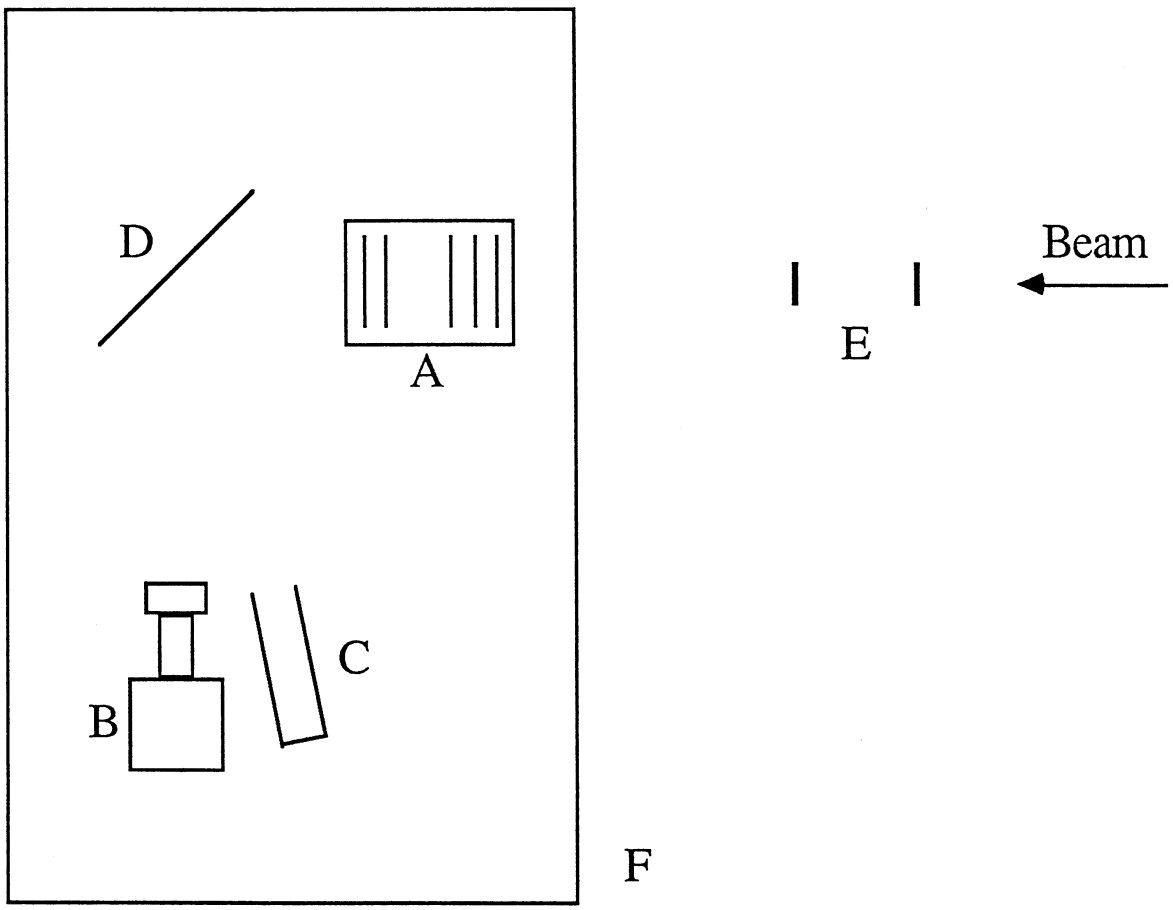

Figure 4

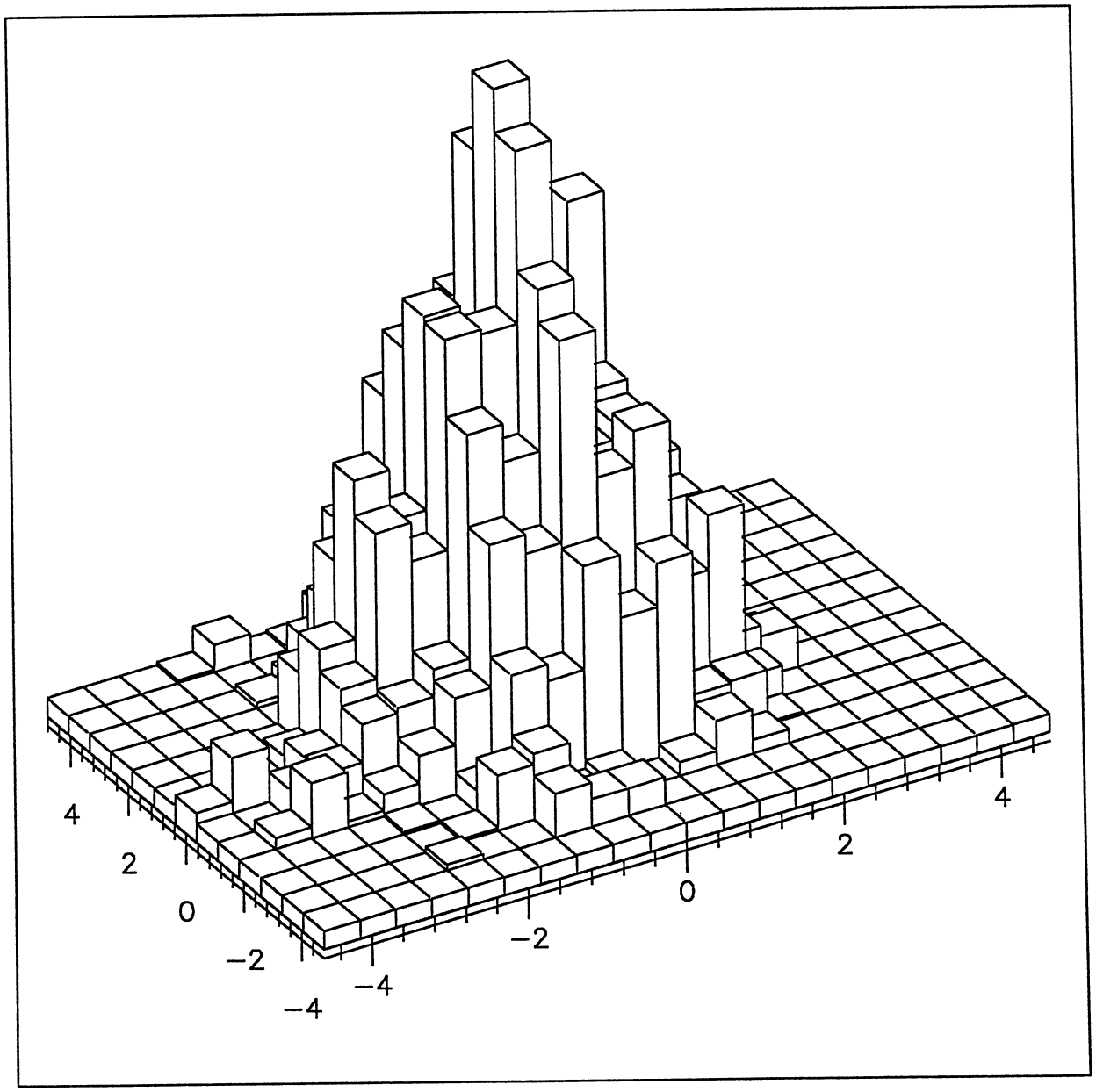

Figure 5

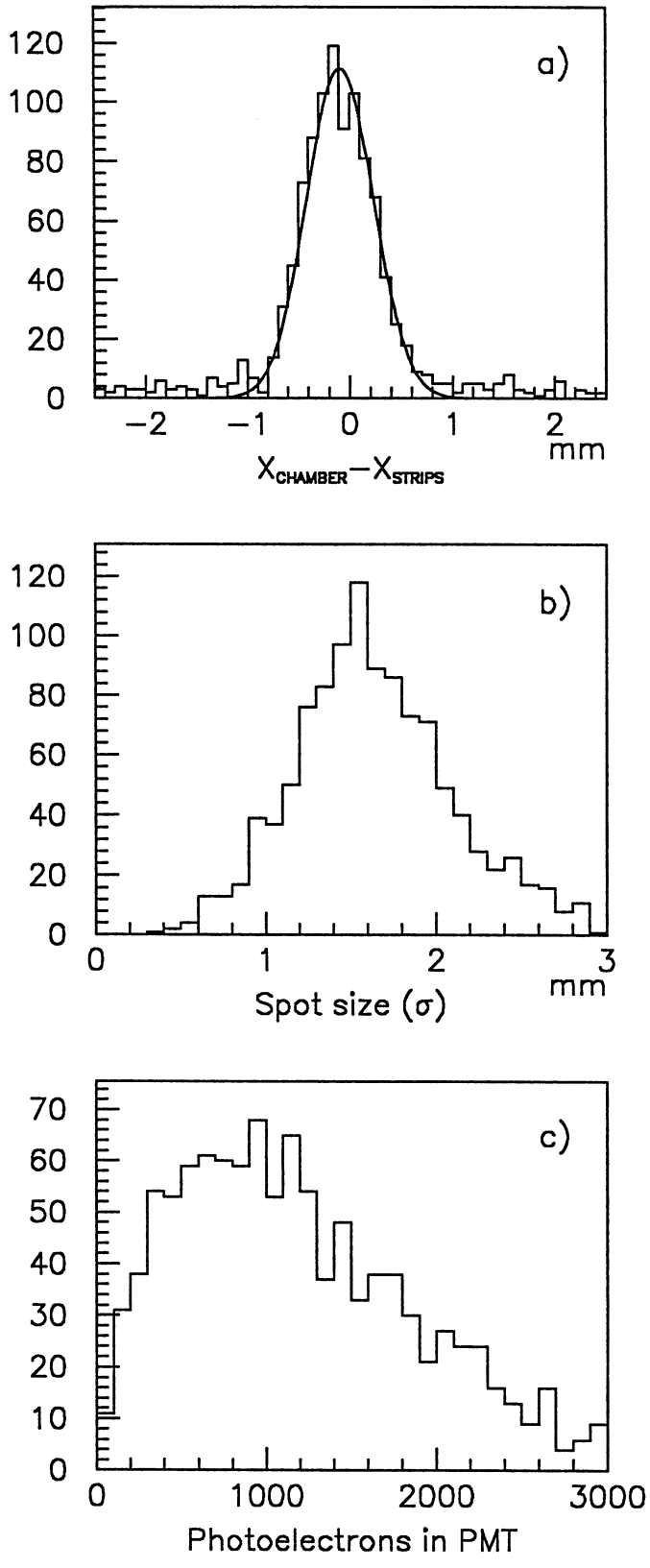
a)
120
100
80
60
40
20
0
−2
−1
0
1
2
mm
$X_{CHAMBER} - X_{STRIPS}$
b)
120
100
80
60
40
20
0
0
1
2
3
mm
Spot size (σ)
c)
70
60
50
40
30
20
10
0
0
1000
2000
3000
Photoelectrons in PMT

Figure 6